Available online at www.sciencedirect.com
ScienceDirect
Catalysis Today 123 (2007) 113–121
CATALYSIS TODAY
www.elsevier.com/locate/cattod

Oxidative dehydrogenation of ethane over Dy_2O_3/MgO supported LiCl containing eutectic chloride catalysts

Balkrishna Tope, Yongzhong Zhu, Johannes A. Lercher *

Technische Universität München, Department of Chemistry, Lichtenbergstraße 4, 85747 Garching, Germany

Available online 2 April 2007

Abstract

The catalytic oxidative dehydrogenation of ethane with alkali and alkaline earth metal chloride modified LiCl supported on Dy_2O_3/MgO (MD) was studied. Eutectic mixtures of alkali and alkaline earth metal chloride with LiCl are formed on the support surface decreasing so the melting point of pure LiCl to temperatures as low as 366 °C (Li-K-MD). All samples had weak basicity decreasing in the order: Li-K-MD < Li-Sr-MD Li-Ba-MD < Li-Na-MD < Li-MD. Physisorbed and chemisorbed CO_2 species are identified for all materials studied by *in situ* IR spectroscopy. Bidentate carbonate species are the most abundant on Li-MD, while on modified samples bi- and unidentate carbonate species exist. The catalyst activity increases with decreasing basicity. Catalyst selectivity increases with increasing reaction temperature and is constant above a threshold temperature. The maximum ethene selectivity is directly correlated with the melting point of the eutectic melt on the catalyst support.

Keywords: Oxidative dehydrogenation (ODH); Eutectic chloride; IR spectroscopy

1. Introduction

Ethene and propylene are important building blocks of the chemical industry being currently produced *via* steam cracking of various petroleum fractions. The mature process is operated under severe conditions with disadvantages including thermodynamic limitations, high energy demand, and formation of coke on the catalyst [1]. The olefin market growing at a rate of 3% per year and the continuous rising fuel costs has spurred substantial interest to develop alternative routes to steam cracking [1–3].

Oxidative dehydrogenation (ODH) of light alkanes is one of the most promising alternatives [1–3]. OHD is exothermic and can be operated at lower temperatures ($T < 650^{\circ}C$) thus reducing the energy input. The feedstock of ODH, light alkanes, is easily available and competitively priced. However, the development of an appropriate catalyst proved to be difficult, since CO_x is thermodynamically favored and the olefins produced are generally more reactive than alkanes. Consequently, catalysts that can activate ethane effectively, while maintaining high ethene selectivity would be highly desirable.

Catalysts that are active for the ODH of alkanes can be grouped into two categories [3]. The first group materials are reducible metal oxides, based on V and Mo oxides, which can operate at temperatures below 550 °C [4–11]. The second group are non-reducible alkali metal-based oxide catalysts that are active at a temperature above 600 °C [12–22]. Li/MgO is perhaps the most prominent system. While unmodified Li/MgO shows moderate activity [12,13], the activity of Li/MgO can be significantly increased by addition of small amounts of chlorine-containing compounds in the feed or by direct incorporation of chlorine into the catalyst [16,17]. The activity of Li/MgO can be further improved by addition of SnO_2, La_2O_3, Nd_2O_3, or Dy_2O_3 as a promoter [18,19]. Ethene yields up to 77% have been obtained when Dy_2O_3 is used as a promoter [19].

From our previous study [19], we found that high selectivity is obtained, once the reaction temperature approaches the melting point of LiCl. To further study this phenomenon and the effect of melting point on the ODH of alkanes, we prepared a series of catalyst by adding alkali and alkaline earth metal chlorides to the LiCl/Dy_2O_3/MgO catalyst. Various physicochemical characterization techniques are used together with the

* Corresponding author. Tel.: +49 89 28913540; fax: +49 89 28913544.
E-mail address: johannes.lercher@ch.tum.de (J.A. Lercher).

0920-5861/$ – see front matter
doi:10.1016/j.cattod.2007.02.020

catalytic tests for the OHD of ethane in order to establish structure–activity relations for chloride containing catalysts.

2. Experimental

2.1. Catalyst preparation

Metal chloride modified $LiCl/Dy_2O_3/MgO$ catalysts were prepared by wet impregnation. Typically, Dy_2O_3 and MgO powders were added to a solution containing $LiNO_3$, HCl, and NH_4Cl (ratio $HCl:NH_4Cl = 1:1$), and one additional metal chloride (NaCl, KCl, $SrCl_2$, and $BaCl_2$). Then, the slurry obtained was stirred at 80 °C for 2 h. Subsequently, the water was evaporated under reduced pressure and the residue was dried at 100 °C. All samples were calcined at 350 °C for 4 h followed by calcination at 600 °C for 4 h, except for the unmodified $LiCl/Dy_2O_3/MgO$ which was calcined at 650 °C. Based on the different metal chloride added, the catalyst was denoted as Li-X-MD (X = Na, K, Sr, and Ba).

In all samples, the atomic ratio of Mg:Dy:Li was 100:2:10. The chloride ion concentration deposited from HCl and NH_4Cl was 20 wt% of MgO. The amount of alkali or alkaline earth metal chloride was added according to eutectic composition with LiCl (see Table 1).

2.2. Physicochemical characterization

The metal cation composition of Li, Na, K, Sr, Ba, Mg, and Dy was analyzed by atomic absorption spectroscopy (AAS). The chloride concentration was analyzed by ion chromatography. The specific surface area was determined by N_2 sorption at 77 K (BET method).

The X-ray diffraction (XRD) was measured with a Philips X'Pert diffractometer using Cu Kα radiation. *In situ* high temperature XRD was recorded in a Parr chamber HTK 1200 under controlled gas atmosphere with a temperature increment of 50 °C.

TG-DSC measurements were performed with a modified Setaram TG-DSC thermoanalyzer with a base pressure of 10^{-5} mbar. The initial amount of each catalyst used for the DSC analyses was approximately 15 mg and the temperature was linearly increased from 100 to 700 °C at a rate of 10 °C/min.

CO_2 temperature-programmed desorption (TPD) was used to determine the basic properties. The measurement was performed in a dedicated UHV setup connected to a quadrupole mass spectrometer (Pfeiffer Vacuum QME 200). The sample was pretreated at 500 °C for 1 h followed by adsorption of CO_2 at 100 °C. After being outgassed for 6 h at 100 °C under 10^{-3} mbar, desorption of CO_2 was monitored by mass spectrometry during heating at a rate of 10 °C/min up to 600 °C.

Infrared spectra of adsorbed CO_2 were recorded on a Bruker IFS 88 FTIR spectrometer with a resolution of 4 cm^{-1}. The sample, about 15 mg, was pressed into a self-supported wafer, pretreated at 500 °C under vacuum ($\sim 10^{-5}$ mbar) for 1 h, and cooled to 30 °C to record a spectrum. The sample was equilibrated with CO_2 at 0.4 and 1 mbar for 1 h before recording the spectra.

Table 1
Eutectic compositions and eutectic melting point

Mixture	Eutectic composition	Eutectic melting point (°C)
LiCl	–	610
LiCl/NaCl	72:28	554
LiCl/KCl	59:41	353
$LiCl/SrCl_2$	64:36	492
$LiCl/BaCl_2$	75:25	514

2.3. Catalytic tests

The catalytic measurements were performed in a tubular fixed-bed quartz reactor. Typically, 300 mg of the catalyst together with the equal amount of SiC of the same particle size was packed in the reactor. The remaining dead volume was filled with pure SiC, and a quartz bar was inserted downstream to reduce the post-catalytic volume. Prior to each run, the sample was heated to 550 °C for 1 h in He followed by a stability test at 550 °C for 2 h in the presence of the reaction mixture. The composition of the reaction mixture was 8% C_2H_6, 8% O_2, and 84% He. The weight hourly space velocity was 0.8 h^{-1}, if not otherwise stated. To study the ethene selectivity of various catalysts at the same conversion level, a series of experiments were performed at constant temperature (550 °C), constant ethane/oxygen ratio (1/1), but at different contact time W/F (0.48–7.72 g s/cm^{-3}).

The oxidative dehydrogenation of ethane was performed in the temperature range 450–600 °C. The reaction products were analyzed *on-line* by a Hewlett Packard 6890 series gas chromatograph equipped with an FID and a TCD detector. A PoraPLOT Q and a Molsieve column were used for product separation. The main reaction products were C_2H_4, CO, CO_2, and water. The conversion of ethane and selectivity of ethene was calculated on a carbon basis. To determine the contribution of gas phase reactions, a separate experiment was performed at 600 °C by using a SiC filled reactor. Under this condition, the ethane conversion was less than 1%, which indicates that the direct gas phase reaction is negligible.

3. Results and discussions

3.1. Chemical compositions and catalyst phases

The elemental composition of the catalysts and the specific surface areas are compiled in Table 2. The atomic ratio of Li/Na, Li/K, Li/Sr, and Li/Ba in the activated samples was identical to the ratio added in the preparation according to the eutectic composition. As chloride was added in excess and the catalyst treatment temperature, 600 °C, was relatively low, it is assumed that alkali and alkaline earth metals are present in the catalysts as chloride salts. Therefore, we conclude that eutectic mixtures of alkali or alkaline earth metal chloride and LiCl are present in the catalysts. The specific surface area of the samples Li-Na-MD, Li-Sr-MD, and Li-Ba-MD decreased slightly compared with Li-MD, while the specific surface area of

Table 2
Catalyst composition and specific surface area

Catalyst	Mg (wt%)	Dy (wt%)	Li (wt%)	Cl (wt%)	Atomic ratio[a]				BET-SSA (m^2/g)
					Li/Na	Li/K	Li/Sr	Li/Ba	
Li-MD	46.7	7.7	1.61	5.1	–	–	–	–	12.4
Li-Na-MD	43.5	5.4	1.44	6.1	2.5(2.6)	–	–	–	9.2
Li-K-MD	42.9	6.8	1.40	6.9	–	1.5(1.5)	–	–	2.1
Li-Sr-MD	43.6	6.3	1.16	5.1	–	–	1.7(1.8)	–	10.0
Li-Ba-MD	41.8	8.7	1.30	7.2	–	–	–	2.9(3.0)	7.3

[a] Value in the bracket is the ratio of bulk metal chloride eutectic mixture.

Li-K-MD decreased dramatically to 2.1 m^2/g. As Li-K-MD has a very low melting point (see DSC measurement), the pores of the sample may be blocked by the LiCl/KCl melt during calcination causing the extremely low specific surface area.

XRD was used to characterize the crystalline phases formed in the calcined catalysts. At room temperature, crystalline LiCl was not observed by X-ray diffraction, as it is strongly hygroscopic. Therefore, the diffractograms of all samples were measured at 100 °C under inert atmosphere. As seen in Fig. 1, MgO was the dominating crystalline phase and crystalline LiCl and DyOCl were also observed in all samples. However, crystalline Dy_2O_3 was not detected. In a separate experiment, we observed Dy_2O_3 diffraction lines, when the catalyst calcination temperatures exceeded 650 °C. Other phases detected are summarized in Table 2. NaCl, KCl, $SrCl_2$, and $BaCl_2$ phases were observed in the samples containing the respective chlorides.

To describe phase transformations under reaction conditions, X-ray diffractograms of pre-activated catalysts were taken *in situ* between 100 and 650 °C. Fig. 2 shows the XRD diffractograms of Li-K-MD catalyst at various temperatures, representative for all Li containing catalysts within this study. MgO was present over the entire temperature range studied (100–650 °C). Diffraction peaks of DyOCl disappeared at 600 °C due to decomposition of DyOCl. It is interesting to note that for all Li containing catalysts the XRD reflexes of the alkali and alkaline earth metal chlorides were shifted to higher *d*-values with increasing temperature. The diffraction peaks of the alkali and alkaline metal chlorides disappeared at different temperatures (see Table 3 and Fig. 2). The diffraction peaks of LiCl and KCl disappeared at approximately 350 °C, a temperature much lower than the melting point of LiCl (mp 610 °C) and KCl (mp 771 °C) indicating that a eutectic mixture of LiCl/KCl was formed.

To investigate the phase transformation in more detail, TG-DSC was used to measure the melting point of the alkali or alkaline earth chloride mixtures with LiCl on the support surface. Fig. 3 shows the DSC signals for all catalysts within the temperature range of 300–650 °C. For pure Li-MD, the observed endothermic signal started to increase at around 550 °C and reached its maximum at 604 °C (minimum in the heat flux), indicating that LiCl is transformed to liquid state. The temperature at the highest endothermic signal corresponded to the melting point of pure LiCl (610 °C). For all other samples, only one phase transformation was observed and the corresponding melting point was much lower than that of LiCl. This is attributed to the formation of eutectic mixtures of alkali or alkaline earth metal chlorides with LiCl. The melting points of the supported chlorides together with the value predicted by thermodynamics at the eutectic composition are shown in Table 3. It can be seen that the phase transformation temperatures perfectly coincide with the melting point of the pure bulk metal chloride mixtures. Thus, we conclude that the addition of alkali or alkaline earth metal chloride lowers the

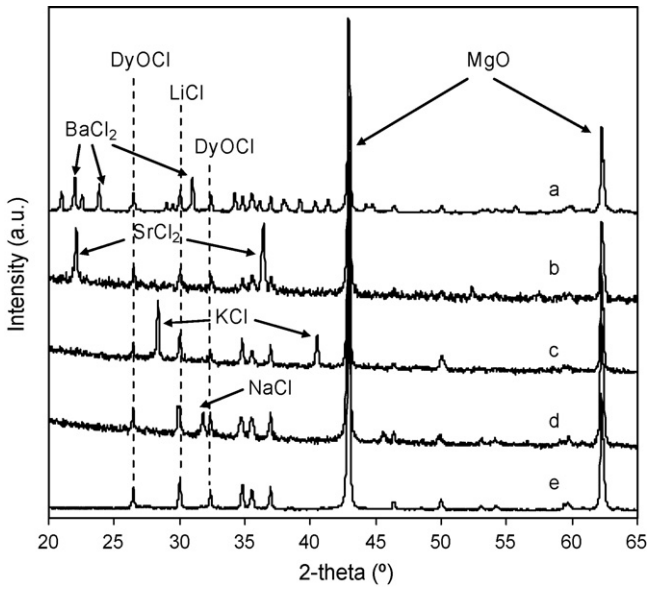

Fig. 1. XRD diffractograms obtained at 100 °C under inert atmosphere: (a) Li-Ba-MD, (b) Li-Sr-MD, (c) Li-K-MD, (d) Li-Na-MD, and (e) Li-MD.

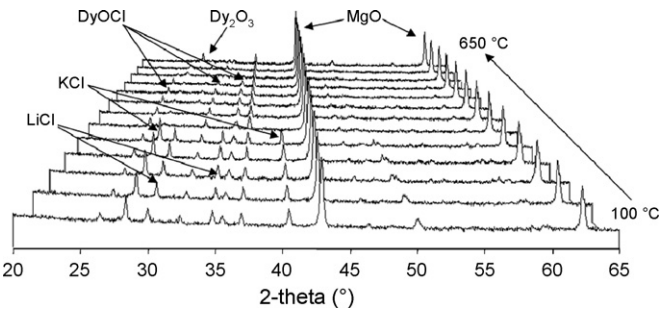

Fig. 2. XRD diffractograms of Li-K-MD measured at different temperatures under inert atmosphere (temperature step, 50 °C).

Table 3
Main crystalline XRD phases at 100 °C, melting point (mp) estimated by *in situ* HT-XRD, and mp determined by DSC

Catalyst	Phases detected by XRD at 100 °C	mp (HT-XRD) (°C)	mp (DSC) (°C)	mp (thermo.)[a] (°C)
Li-MD	MgO, DyOCl, LiCl	550–650	604	610
Li-Na-MD	MgO, DyOCl, LiCl, NaCl	500–600	560	554
Li-K-MD	MgO, DyOCl, LiCl, KCl	350–400	366	353
Li-Sr-MD	MgO, DyOCl, LiCl, $SrCl_2$	450–500	494	492
Li-Ba-MD	MgO, DyOCl, LiCl, $BaCl_2$	500–550	524	514

[a] Thermodynamic eutectic melting point of the bulk binary mixtures of alkali or alkaline metal chloride with LiCl.

melting point of the supported phase compared to $LiCl/Dy_2O_3/MgO$.

3.2. Acid–base properties of the catalysts

3.2.1. Temperature-programmed desorption of adsorbed CO_2

CO_2 is a suitable probe molecule to determine the basicity of solid catalysts [13,23]. CO_2 physisorbs and chemisorbs on the surface of a basic solid catalyst. To eliminate the influence of physisorption, all samples were evacuated after adsorption of CO_2 at 100 °C for 6 h. After this treatment, the desorption peak detected by TPD was assigned to CO_2 chemisorbed in the form of carbonates. From the TPD profiles in Fig. 4, only one broad desorption peak was identified for all samples. On the higher temperature side, however, a broadening of the TPD peak was observed. This indicates that different adsorption species were present and contributed to the desorption of CO_2. As shown in Table 3, the total amount CO_2 desorbed was relatively small indicating that the presence of the chloride ions limits the adsorption of CO_2. The amount of CO_2 desorbed increased in the order: Li-MD < Li-Na-MD < Li-Ba-MD ≈ Li-Sr-MD < Li-K-MD. In addition, the temperatures of the desorption maximum were higher for Li-K-MD, Li-Ba-MD, and Li-Sr-MD than for Li-MD and Li-Na-MD. This indicates that first three samples have a higher base strength than the latter two.

3.2.2. Infrared spectra of adsorbed CO_2

The IR spectrum of adsorbed CO_2 is used to characterize Lewis acid and base sites on metal oxides and zeolites. Three types of bands have been observed varying with the nature of the interaction of CO_2 with the catalyst surface [24–27]. These bands include the asymmetric stretching of adsorbed CO_2 (ν_3) and the carbonate vibrations between 1800 and 1200 cm^{-1}. The IR spectra of adsorbed CO_2 on alkali or alkaline earth metal chloride modified $LiCl/Dy_2O_3/MgO$ catalysts are shown in Fig. 5. The asymmetric vibrations due to molecularly adsorbed CO_2 on Li-MD, Li-Na-MD, Li-Ba-MD, Li-Sr-MD, and Li-K-MD appeared at 2358, 2352, 2350, 2347, and 2344 cm^{-1}, respectively. The ν_3 vibration shifts to lower wavenumbers as the ionic radius of the alkali and alkaline earth metal cation increases. This shift is related to the electron pair acceptor strength of the metal cations towards adsorbed CO_2. It implies that the acid strength of the accessible cations decreases in the order Li-MD > Li-Na-MD > Li-Ba-MD > Li-Sr-MD > Li-K-MD. The sequence inversely tracks the increase in interaction with CO_2 observed by TPD of CO_2. It is interesting to note that the sequence of acid strength does not follow exactly the trend expected from the electronegativity of the cations. This is attributed to the varying concentrations of cations needed to achieve the eutectic mixture and suggests that the individual nature of the cations is important for the stability of the carbonate formed.

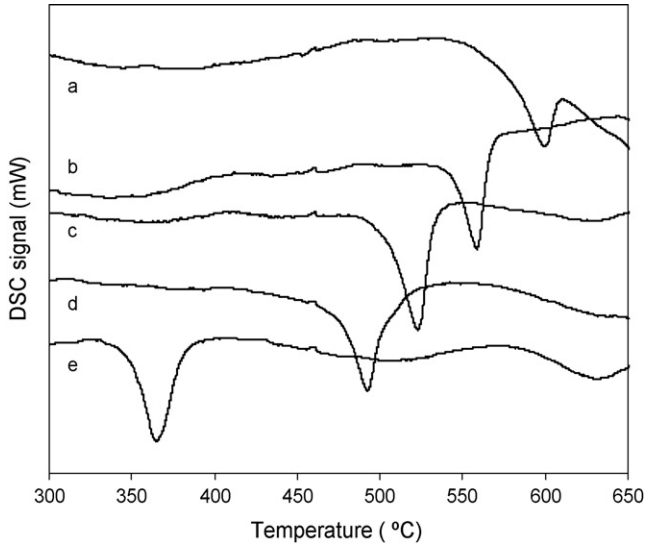

Fig. 3. TG-DSC analysis of calcined samples: (a) Li-MD, (b) Li-Na-MD, (c) Li-Ba-MD, (d) Li-Sr-MD, and (e) Li-K-MD.

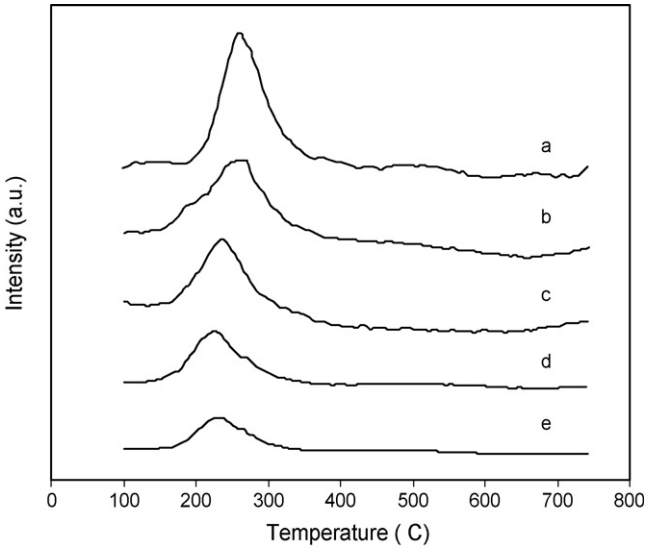

Fig. 4. TPD of adsorbed CO_2: (a) Li-K-MD, (b) Li-Sr-MD, (c) Li-Ba-MD, (d) Li-Na-MD, and (e) Li-MD.

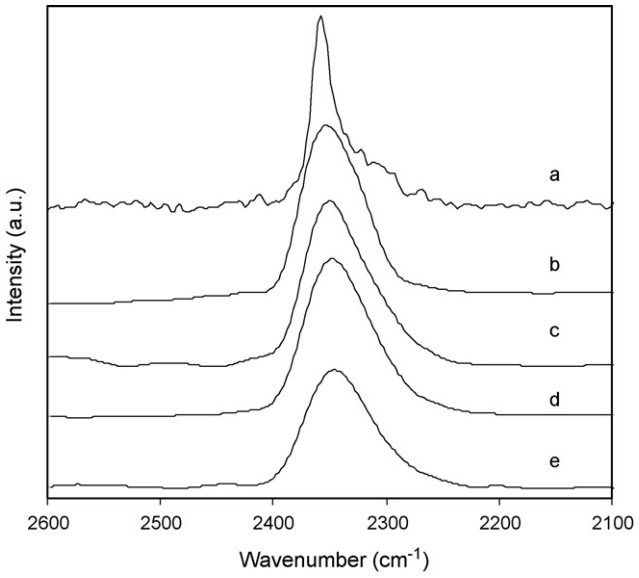

Fig. 5. IR spectra of adsorbed CO_2 (0.4 mm equilibrium pressure of CO_2) in the asymmetric stretching region: (a) Li-MD, (b) Li-Na-MD, (c) Li-Ba-MD, (d) Li-Sr-MD, and (e) Li-K-MD.

Fig. 6 shows the IR spectra of the modified and unmodified $LiCL/Dy_2O_3/MgO$ samples after CO_2 adsorption and subsequent evacuation at 30, 200, and 400 °C. The unmodified sample, Li-MD, exhibits two bands at 1340 and 1620 cm^{-1}, respectively. The former is assigned to the symmetric O–C–O stretching, the to the latter asymmetric O–C–O stretching vibration. Both are typical vibration modes of bidentate carbonate species formed on Lewis-acid–Brønsted-base pairs (Mg^{2+}–O^{2-} pair site, where M^+ is the metal cation Mg^{2+} or alkali or alkaline metal cation) [28]. Bidentate carbonate species dominate on Li-MD. As the temperatures increase, the intensities of these bonds decrease suggesting that the bidentate carbonate species are not stable and in consequence, the basic sites on Li-MD are of moderate strength.

For the modified samples, the IR spectra are more complex. In addition to the bidentate carbonate species, unidentate carbonate species are also detected. Especially for Li-K-MD, Li-Sr-MD, and Li-Ba-MD, vibration bands at 1380–1400 cm^{-1}, assigned to symmetric O–C–O stretching and vibration bands at 1500–1530 cm^{-1}, assigned to asymmetric O–C–O stretching, appear in their spectra. These bands can be ascribed to the unidentate carbonate species which form on isolated surface O^{2-} ions [28]. At higher temperatures, the CO_2 bands shift to the unidentate carbonate position suggesting that the unidentate carbonate species are more stable than the bidentate carbonate species. This indicates higher base strength on the surface of these modified compared to the other samples.

The relative intensity of carbonate bands decreased with decreasing equilibrium pressure, but the bands persisted even after evacuation to 10^{-5} mbar (see Table 4). The integrated value of the intensities of the bands in the range 1800–1200 cm^{-1} on the different samples increased in the order: Li-MD < Li-Na-MD < Li-Ba-MD < Li-Sr-MD < Li-K-MD. This indicates that the base site density increases assuming that the molar extinction coefficient does not vary between these samples.

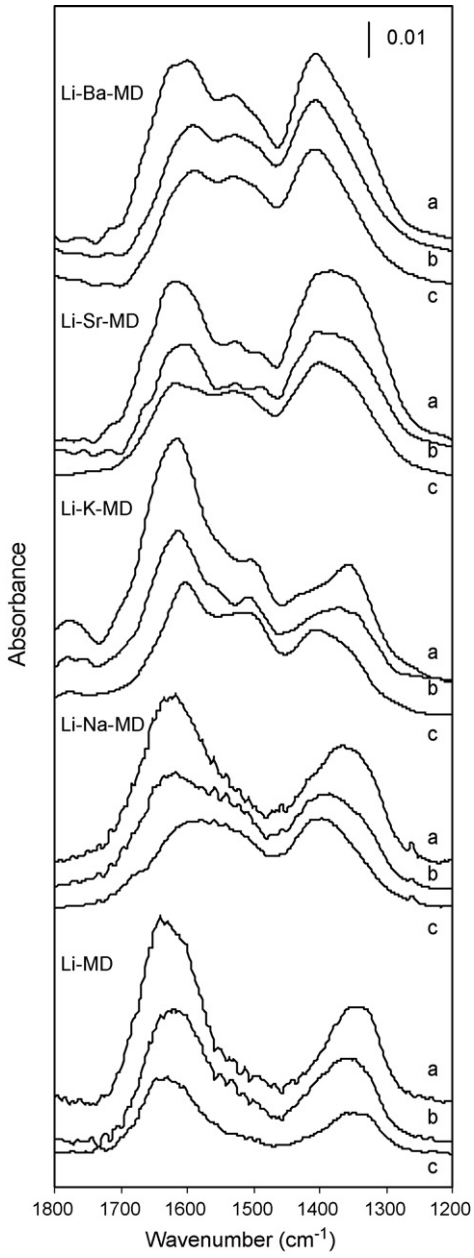

Fig. 6. IR spectra of adsorbed CO_2 on Li-M-MD catalysts and desorbed under vacuum at different temperatures: (a) 30 °C, (b) 200 °C, and (c) 400 °C.

3.3. Catalytic activity for ODH of ethane

Ethene, CO, CO_2, and H_2O were the main reaction products during the oxidative dehydrogenation of ethane. The ethane conversion and the ethene yield are presented in Figs. 7 and 8 as a function of the reaction temperature. At the same temperature, the highest activity was found for Li-MD, the lowest for Li-K-MD, and the activities of other samples were in between. For example, at 580 °C, the ethane conversion was 73% over Li-MD, 46% over Li-Na-MD, 27% over Li-K-MD, 44% over Li-Sr-MD, and 40% over Li-Ba-MD. The corresponding

Table 4
Strength and concentration of basic sites derived from TPD of CO_2 and the relative concentration of base sites derived from IR spectra of adsorbed CO_2

Catalyst	TPD		IR spectroscopy	
	Temperature of peak max (K)	CO_2 adsorbed (mmol/g)	Relative intensity at CO_2 pressure[a]	
			1 mbar	0.4 mbar
Li-MD	234	0.16	81	74
Li-Na-MD	234	0.18	95	82
Li-Ba-MD	244	0.22	102	88
Li-Sr-MD	257	0.22	116	95
Li-K-MD	262	0.23	120	108

[a] Integrated intensities of the bands in the range 1800–1200 cm^{-1}.

selectivity to ethene was 80% (Li-MD), 86% (Li-Na-MD), 96% (Li-K-MD), 91% (Li-Sr-MD), and 88% (Li-Ba-MD). This indicates that addition of the metal chlorides caused a decrease in catalytic activity and an increase in selectivity.

The effect of temperature on the selectivity of ethene is shown in Fig. 9. Li-K-MD presented the highest selectivity and its selectivity was retained at around 96% in the temperature range from 450 to 595 °C. For other catalysts, the ethene selectivity increased with temperature and then became constant, when the temperature approached a certain value. A further increase of the temperature did not change the product distribution. It is important to note that the temperature, at which the high and constant selectivity was obtained, coincides with the temperatures at which spreading/melting of the alkali and alkaline earth metal chloride phases was experimentally observed.

It is also remarkable that the lower melting points induce higher ethene selectivity. By adding alkali or alkaline earth metal chloride, the constant ethene selectivity increased from 80% for Li-MD to 96% for Li-K-MD. The possible reasons for the effect of melting point on the ethene selectivity is speculated to be related to the easier desorption of ethyl radicals formed on the catalyst surface and weaker adsorption of ethene in molten state.

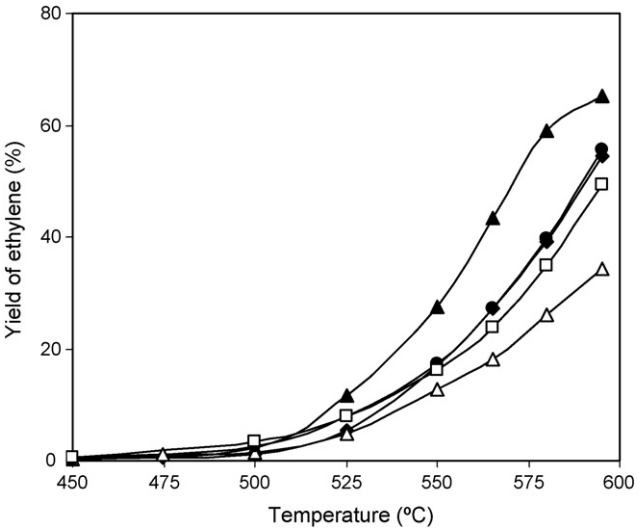

Fig. 8. Yield of ethene at different temperatures over: (▲) Li-MD, (◆) Li-Na-MD, (△) Li-K-MD, (●) Li-Sr-MD, and (□) Li-Ba-MD.

A suitable ethane ODH catalyst should be able to convert ethane to ethene effectively, while maintaining high selectivity to ethene. Thus, the selectivity of various alkali or alkali earth metal chloride modified LiCl catalysts was explored at constant temperature (550 °C), constant ethane/oxygen ratio (1/1), but at different contact time W/F (0.48–7.72 g s/cm^{-3}). The ethene selectivity as a function of ethane conversion is shown in Fig. 10. From this figure, it is obvious that Li-K-MD has the highest selectivity at the same conversion level and the ethene selectivity over various catalyst following the order Li-K-MD > Li-Sr-MD > Li-Ba-MD > Li-Na-MD > Li-MD. This order can be correlated with the melting point of eutectic mixtures on the support. The lower the melting point, the higher the selectivity is. It is also noted that the selectivity for all catalysts decreases only a slightly at conversions below 78%,

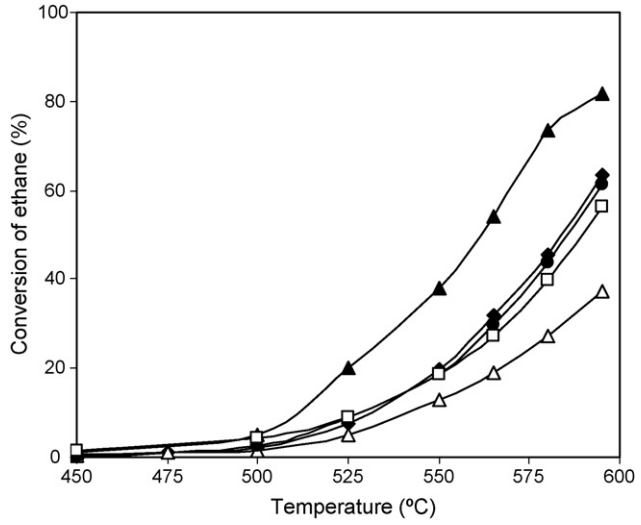

Fig. 7. Conversion of ethane at different temperatures over: (▲) Li-MD, (◆) Li-Na-MD, (△) Li-K-MD, (●) Li-Sr-MD, and (□) Li-Ba-MD.

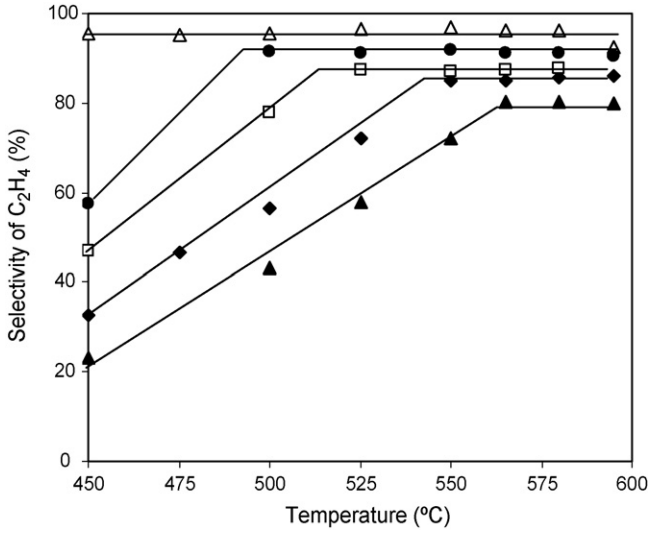

Fig. 9. Selectivity of ethene at different temperatures over: (▲) Li-MD, (◆) Li-Na-MD, (△) Li-K-MD, (●) Li-Sr-MD, and (□) Li-Ba-MD.

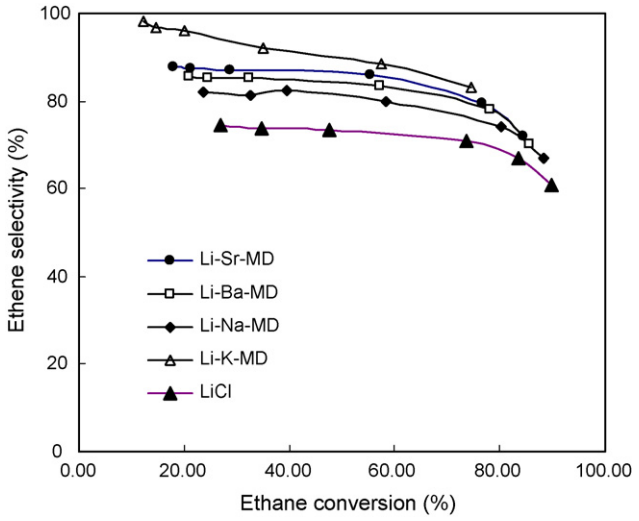

Fig. 10. Ethene selectivity as a function of ethane conversion at 550 °C with a C_2H_6/O_2 ratio of 1:1.

indicating only a minor influence of secondary reactions. Above 78% conversion, the selectivity decreased markedly at the expense of an increase in CO_x.

4. Discussion

It has been concluded that the unusually high selectivity for oxidative dehydrogenation of ethane over LiCl based catalysts is related to the molten state of LiCl in the active catalyst [19]. Thus, it is a logical step to explore other low melting eutectic mixtures with respect to these properties and to relate the acid/base properties of these materials to the activity and selectivity for oxidative dehydrogenation of ethane. In order to prepare practical catalysts, the molten salts have to be supported on a relatively inert support, forming a thin layer on its surface. In this contribution, we report the preparation, characterization, and catalytic properties of such supported binary eutectic mixtures of LiCl with alkali and alkaline earth metal chlorides.

Let us establish first that the eutectic mixture exists on the catalyst and that it is molten under reaction conditions. Indirect evidence for the existence of the molten eutectic mixture comes from the elemental analysis. The atomic ratio of Li/Na, Li/K, Li/Sr, and Li/Ba (see Table 2) agrees well with that of the composition suggested by the thermodynamic composition of the eutectic mixture. More direct evidence is provided by *in situ* high temperature XRD. In the XRD diffractograms, the XRD peaks of the alkali or alkaline metal chlorides shifted to higher *d*-values with increasing temperature (Fig. 2) and disappeared finally at a certain temperature (Table 3, Fig. 3). This indicates an expansion of the corresponding alkali or alkaline metal chloride lattice as well as spreading and/or melting of the metal chloride crystallites at the catalyst surface at a defined temperature. Most important is that the theoretical melting points of pure bulk LiCl, LiCl/NaCl, LiCl/KCl, LiCl/$SrCl_2$, and LiCl/$BaCl_2$ are within the estimated melting temperature regions, determined by the disappearance of XRD diffraction peaks (Table 3). Thus, it is concluded that the disappearing peaks are affiliated with the melting of the solid metal chloride phases. Calorimetry provides the most direct conclusive evidence (see Fig. 3), as the onset temperature and melting point can be clearly observed. The melting points of all samples determined by calorimetry coincide perfectly with those reported in the literature [29]. Taking all three pieces of evidence together, it is safe to conclude that indeed the supported eutectic melt has been formed on the MgO surface.

The effect of supported eutectic melt on catalytic activity was studied for the ODH of ethane. The catalytic experiments (see Figs. 7 and 8) indicate that the addition of alkali or alkaline earth metal cations decreased the catalytic activity, but increased the selectivity. To explore the reasons, the acid–base properties of these materials were determined by TPD and by IR spectra of adsorbed CO_2. The TPD of CO_2 (Fig. 4) indicates that the addition of alkali and alkali earth metal cations leads to stronger adsorption of CO_2. The IR spectra of linearly adsorbed CO_2 shows, however, that the addition of alkali and alkali earth metal cations decreases the strength of the accessible Lewis acid sites. Thus, both experiments (see Table 4) complementarily suggest that the acid strength of the accessible Lewis acid sites increases, while the base strength of samples decreases in the order Li-K-MD < Li-Sr-MD < Li-Ba-MD < Li-Na-MD < Li-MD. So, the introduction of metal cations with low electronegativity such as Na^+, K^+, Sr^{2+}, and Ba^{2+} leads to a more basic surface, while the acid strength of the action decreases. Both experiments also suggest that the original MgO surface covered to a significant fraction with the melt, but that oxide fractions are either still available or that parts of the chloride is converted back to surface carbonates. It is worth noting that with increasing size of the cation, CO_2 tends to form more unidentate carbonates (see Fig. 6). As this seems to be more stable, strongly adsorbed CO_2 may block some active sites, and thus lowering catalytic activity.

Thus, while we note that the stronger Lewis acid cations lead to higher catalytic activity, we cannot rule out that the poisoning of CO_2 is the cause of lower activity of the more basic catalyst, i.e., those with a lower eutectic melting temperature. Lunsford and coworkers [16,17], who had used Cl^- as a modifier reached such a conclusion when studying the influence of the surface acid/base properties of Li^+–MgO–Cl^- in the ODH of ethane.

Contrary to the effect on catalytic activity, addition of alkali or alkaline metal chloride has a remarkable positive effect on the catalyst selectivity. As shown in Fig. 9, the ethene selectivity increased with the increasing temperature, when the reaction temperatures were below melting point. Once the reaction temperature approached or exceeded the chloride melting point, constant selectivity was obtained and maintained up to 595 °C. Remarkably, the level of this constant ethene selectivity is directly correlated with the melting point of the catalyst (Fig. 11). Catalysts with a lower melting point have a higher selectivity. Swaan et al. [20] reported that a Li/Na/MgO catalyst showed a selectivity of 86% to ethene at 38% conversion for the ODH of ethane while the Li/MgO catalyst showed a selectivity of 80% at the similar conversions. The authors speculated that the increased

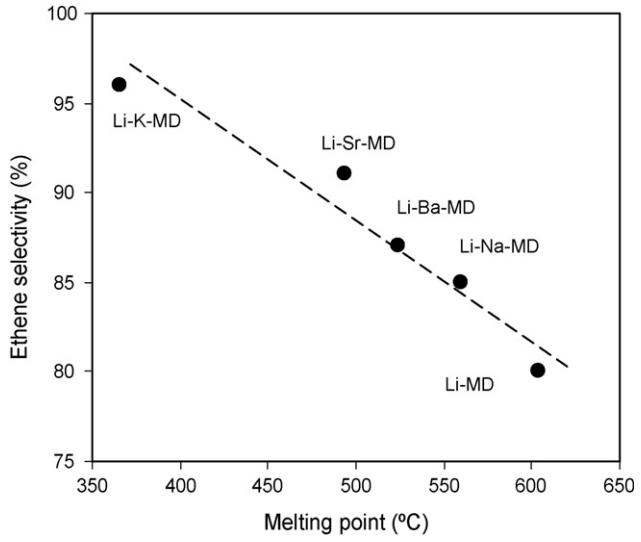

Fig. 11. Correlation between the melting point of the eutectic melt and the maximum ethene selectivity.

selectivity over Li/Na/MgO catalyst is related to a molten layer of $LiNaCO_3$ forming a eutectic with a melting temperature of 490 °C. Thus, it seems that the liquid state under reaction conditions has a beneficial effect on the catalyst selectivity whatever the active phase may be. Tentatively, we attribute the higher selectivity of the molten catalysts to weaker adsorption of ethene on the mobile surface, which in turn suppresses further oxidation of the formed olefins. In essence, the mobility of exposed cations will reduce the strength of bonding to the double bond of the olefin. The diffusion of the alkali metal cations from the surface into the bulk is suggested to lead to the weakening in the π–C_2H_4–Me^+ interaction, as ethene has a very low solubility in the polar melt. It should be noted that for the supported salts studied, the lower the melting point the weaker the π–C_2H_4–Me^+ interaction.

In our previous paper [19], a radical-based mechanism for the halide-mediated oxidative dehydrogenation of ethane to ethylene is proposed. The hypochlorite [OCl^-], which is formed through oxidizing Cl^- by O_2 solved in the LiCl melt, is postulated to be the active species of the catalyst. Essentially, the same mechanism applies to the catalytic process in this work. Addition of another alkali or alkali earth metal chloride modifies the catalyst acid–base properties and most importantly the melting point of the molten chloride phase can be greatly decreased. The mobility of the cations and anions increases dramatically in the chloride molten phases and hence facilitates desorption of the product ethene and limits the further oxidation of ethene to other undesired by-products. Therefore, it is concluded that lower melting point is beneficial to the catalytic selectivity. The present results do not suggest that the eutectic mixtures change the elementary steps of catalytic ethane activation and formation of ethene. The melt, however, seems to remove all defect sites at the surface and make desorption of ethene easier and enable more oxygen dissolved at lower temperatures forming a transient hypochloride species.

5. Conclusion

Addition of alkali or alkaline earth metal chloride to the $LiCl/Dy_2O_3/MgO$ catalyst markedly affects the melting point as well as the acid and base strength. Direct and indirect physicochemical characterizations suggest that a eutectic melt is formed with all combinations. In practice, alkali or alkaline earth metal chloride addition to supported LiCl leads to a much lower melting point compared to pure supported LiCl.

In parallel TPD of adsorbed CO_2 showed that these additions lead to samples with moderate to weak base strength, its strength decreasing in the order Li-K-MD < Li-Sr-MD < Li-Ba-MD < Li-Na-MD < Li-MD. IR spectra of molecularly adsorbed CO_2 show that that the Lewis acid strength increased in that order. Chemisorbed CO_2 was found to be stabilized as unidentate and bidentate carbonate species on the modified catalysts.

The catalysts containing additional alkali and alkaline earth metal chlorides show lower activity for ODH of ethane than the parent Li-MD. However, they had very high ethene selectivity reaching a constant and high level once the reaction temperatures exceed the melting point. A direct correlation between this constant selectivity and melting point is observed, i.e., the lower the melting point the higher the selectivity is. The high selectivity is concluded to be related to the easier desorption of ethene formed on the catalyst surface. In parallel, however, the activity of the catalysts decreases, which is attributed to the larger and weaker metal cations involved in the modified catalysts and to the poisoning of the more stable carbonates.

Acknowledgments

Partial support for this project from the ‘‘Verband der Chemischen Industrie’’ is gratefully acknowledged. This project has been conducted in parts in the framework of NMP3-CT-2005-011730 IDECAT WP5.

References

[1] M.M. Bhasin, J.H. McCain, B.V. Vora, T. Imai, P.R. Pujado, Appl. Catal. A: Gen. 221 (2001) 397.
[2] M.A. Banares, Catal. Today 51 (1999) 319.
[3] F. Cavani, F. Trifiro, Catal. Today 24 (1995) 307.
[4] P. Botella, A. Dejoz, J.M.L. Nieto, P. Concepcion, M.I. Vazquez, Appl. Catal. A: Gen. 298 (2006) 16.
[5] P. Botella, E. Garcia-Gonzalez, A. Dejoz, J.M.L. Nieto, M.I. Vazquez, J. Gonzalez-Calbet, J. Catal. 225 (2004) 428.
[6] J.M.L. Nieto, P. Botella, M.I. Vazquez, A. Dejoz, Chem. Commun. (2002) 1906.
[7] D. Siegel, J. Biophys. 45 (1986) 399.
[8] E.M. Thorsteinson, T.P. Wilson, F.G. Young, P.H. Kasai, J. Catal. 52 (1978) 116.
[9] W. Ueda, N.F. Chen, K. Oshihara, Chem. Commun. (1999) 517.
[10] E. Heracleous, A.A. Lemonidou, J. Catal. 237 (2006) 162.
[11] E. Heracleous, A.F. Lee, K. Wilson, A.A. Lemonidou, J. Catal. 231 (2005) 159.
[12] E. Morales, J.H. Lunsford, J. Catal. 118 (1989) 255.
[13] J.A. Roos, S.J. Korf, R.H.J. Veehof, J.G. van Ommen, J.R.H. Ross, Catal. Today 4 (1989) 441.

[14] J.B.M.S.S. Hong, Catal. Lett. 40 (1996) 1.
[15] S. Sugiyama, N. Kondo, K. Satomi, H. Hayashi, J.B. Moffat, J. Mol. Catal. A: Chem. 95 (1995) 35.
[16] S.J. Conway, J.H. Lunsford, J. Catal. 131 (1991) 513.
[17] D.J. Wang, M.P. Rosynek, J.H. Lunsford, J. Catal. 151 (1995) 155.
[18] S.J. Conway, D.J. Wang, J.H. Lunsford, Appl. Catal. 79 (1991) L1.
[19] S. Gaab, M. Machli, J. Find, R.K. Grasselli, J.A. Lercher, Top. Catal. 23 (2003) 151.
[20] H.M. Swaan, A. Toebes, K. Seshan, J.G. van Ommen, J.R.H. Ross, Catal. Today 13 (1992) 629.
[21] S.B. Wang, K. Murata, T. Hayakawa, S. Hamakawa, K. Suzuki, Catal. Lett. 62 (1999) 191.
[22] S.B. Wang, K. Murata, T. Hayakawa, S. Hamakawa, K. Suzuki, Chem. Commun. (1999) 103.
[23] J.A. Lercher, C. Gründling, G. Eder-Mirth, Catal. Today 27 (1996) 353.
[24] R. Bal, B.B. Tope, T.K. Das, S.G. Hegde, S. Sivasanker, J. Catal. 204 (2001) 358.
[25] F. Solymosi, H. Knozinger, J. Catal. 122 (1990) 166.
[26] S.B. Waghmode, R. Vetrivel, S.G. Hegde, C.S. Gopinath, S. Sivasanker, J. Phys. Chem. B 107 (2003) 8517.
[27] J.A. Lercher, C. Colombier, H. Noller, Z. Phys. Chem. NF 131 (1982) 111.
[28] V.K. Díez, C.R. Apesteguia, J.I. Di Cosimo, J. Catal. 240 (2006) 235.
[29] Gmelins Handbuch der anorganischen Chemie, 8. Aufl., Lithium, System-Nr. 20, Verlag Chemie, Weinheim, (1974).